JOC The Journal of Organic Chemistry

Article

pubs.acs.org/joc

Ligand-Controlled Reactivity, Selectivity, and Mechanism of Cationic Ruthenium-Catalyzed Hydrosilylations of Alkynes, Ketones, and Nitriles: A Theoretical Study

Yun-Fang Yang,[†,§] Lung Wa Chung,*[,‡] Xinhao Zhang,[†] K. N. Houk,*[,§] and Yun-Dong Wu*[,†,∥]

[†]Lab of Computational Chemistry and Drug Design, Laboratory of Chemical Genomics, Peking University Shenzhen Graduate School, Shenzhen 518055, China

[‡]Department of Chemistry, South University of Science and Technology of China, Shenzhen 518055, China

[§]Department of Chemistry and Biochemistry, University of California, Los Angeles, California 90095, United States

[∥]College of Chemistry and Molecular Engineering, Peking University, Beijing 100871, China

Supporting Information

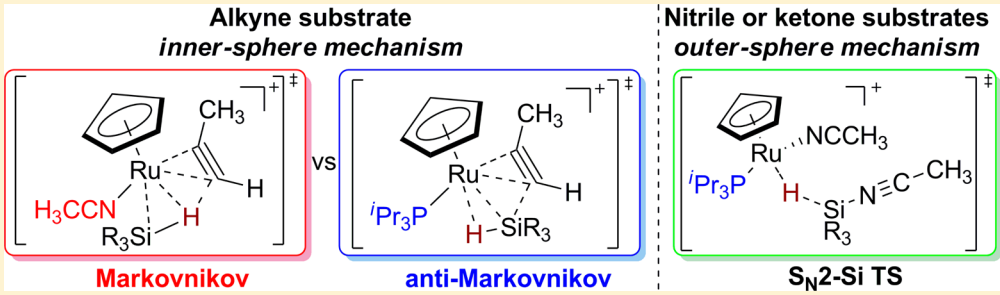

ABSTRACT: Density functional theory calculations with the M06 functional have been performed on the reactivity, selectivity, and mechanism of hydrosilylations of alkynes, ketones, and nitriles catalyzed by cationic ruthenium complexes $[CpRu(L)(MeCN)_2]^+$, with L = P^iPr_3 or MeCN. The hydrosilylation of alkynes with L = P^iPr_3 involves an initial silyl migration mechanism to generate the anti-Markovnikov product, in contrast to the Markovnikov product obtained with L = MeCN. The bulky phosphine ligand directs the silyl group to migrate to C_β of the alkyne. This explains the anti-Markovnikov selectivity of the catalyst with L = P^iPr_3. By contrast, the silane additions to either ketone or nitrile proceed through an ionic S_N2-Si outer-sphere mechanism, in which the substrate attacks the Si center. The P^iPr_3 ligand facilitates the activation of the Si−H bond to furnish a η^2-silane complex, whereas a η^1-silane complex is formed for the MeCN ligand. This property of the phosphine ligand enables the catalytic hydrosilylation of ketones and nitriles in addition to that of alkynes.

INTRODUCTION

Transition metal-catalyzed hydrosilylations have emerged as a powerful methodology for the production of various organosilicon products such as silicon-containing polymers and ceramic materials.[1] Metal-catalyzed alkyne hydrosilylation is the most straightforward and atom-economical method to afford vinylsilanes, which are very useful building blocks in synthetic transformations.[1] Catalytic hydrosilylations of other unsaturated compounds such as carbonyls and nitriles are also of great value in organic synthesis, since these reactions provide protected alcohols and imines.[2] Catalytic hydrosilylation of nitriles to produce the silylaldimines is a great synthetic challenge, as the silylaldimine product is usually more reactive than that of nitriles and leads to further transformations.[3] Most of the nitrile hydrosilylation reactions are also stoichiometric, and only a few catalytic cases have been reported.[4]

Ligands (L) with different steric and electronic properties are known to play an important role in metal−ligand (M−L) bonding as well as structures of transition metal complexes.[5] Different ligands can control reactivity and selectivity in hydrosilylation reactions shown in Scheme 1. For instance, the different regio- and stereoselectivities of hydrosilylation of silyl-substituted alkynes can be changed by using Cp* or Cp ligand.[6] The rhodium-catalyzed intramolecular alkene hydrosilylation of homoallyl silyl ethers gives different regioselectivities with 2,2′-bis(diphenylphosphino)-1,1′-binaphthyl (BINAP) or 1,6-bis(diphenylphosphino)hexane (dpph) ligand.[7]

Trost and Ball reported that a cationic ruthenium complex **1-N** produces branched Markovnikov products from terminal alkynes, as shown in Scheme 2.[8] The classical and modified Chalk−Harrod mechanisms[9] start with an oxidative addition of silane to the metal. In the Chalk−Harrod mechanism, hydride migration occurs first, whereas in the modified Chalk−Harrod mechanism, silyl migration occurs first. A theoretical study by

Received: July 29, 2014
Published: August 26, 2014

   dx.doi.org/10.1021/jo501730n | J. Org. Chem. 2014, 79, 8856−8864

Scheme 1. Ligand-Controlled Regioselective Hydrosilylation Reactions

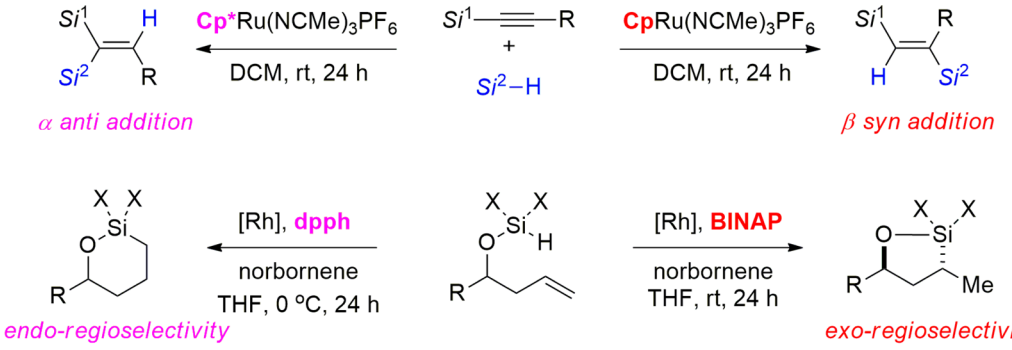

Scheme 2. Hydrosilylation with Cationic Ruthenium Complexes $[CpRu(^{i}Pr_3P)(MeCN)_2]^+$ (1-P) and $[CpRu(MeCN)_3]^+$ (1-N)

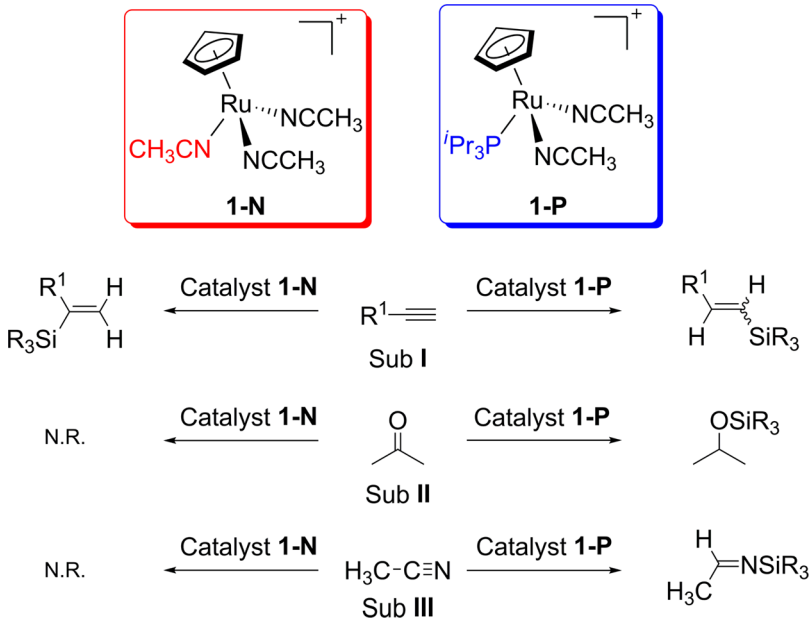

Scheme 3. Inner- and Outer-Sphere Mechanisms of Catalytic Hydrosilylation with Cationic Ruthenium Complexes

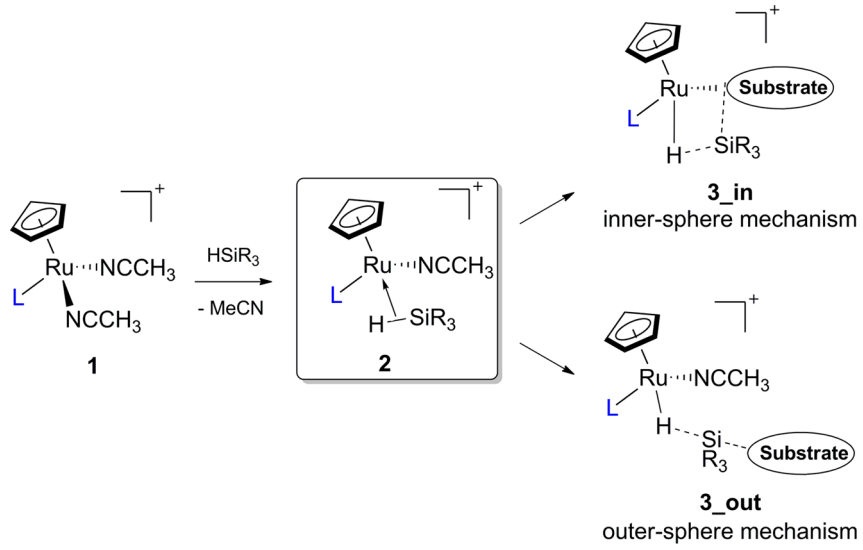

Wu and Trost predicted a new mechanism (the Wu−Trost mechanism) involving an unusual metallocyclopropene intermediate that undergoes reductive silyl migration to the carbene; this rationalizes the unexpected regio- and stereoselectivity of this reaction.[10] In addition, a few recent experiments supported or implicated the Wu−Trost mechanism.[11] In 2010, Nikonov

dx.doi.org/10.1021/jo501730n | J. Org. Chem. 2014, 79, 8856−8864

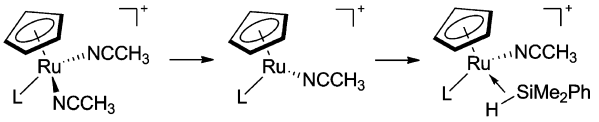

		1-L	1'-L	2-L
L = P^{i}Pr$_3$	ΔG_{gas}	0.0	14.8	7.3
	ΔG_{sol}	0.0	7.3	5.3
L = MeCN	ΔG_{gas}	0.0	14.7	12.5
	ΔG_{sol}	0.0	7.5	11.7

Figure 1. Comparison of ruthenium complexes **1**, **1′**, and **2**. The relative free energies are given in kilocalories per mole.

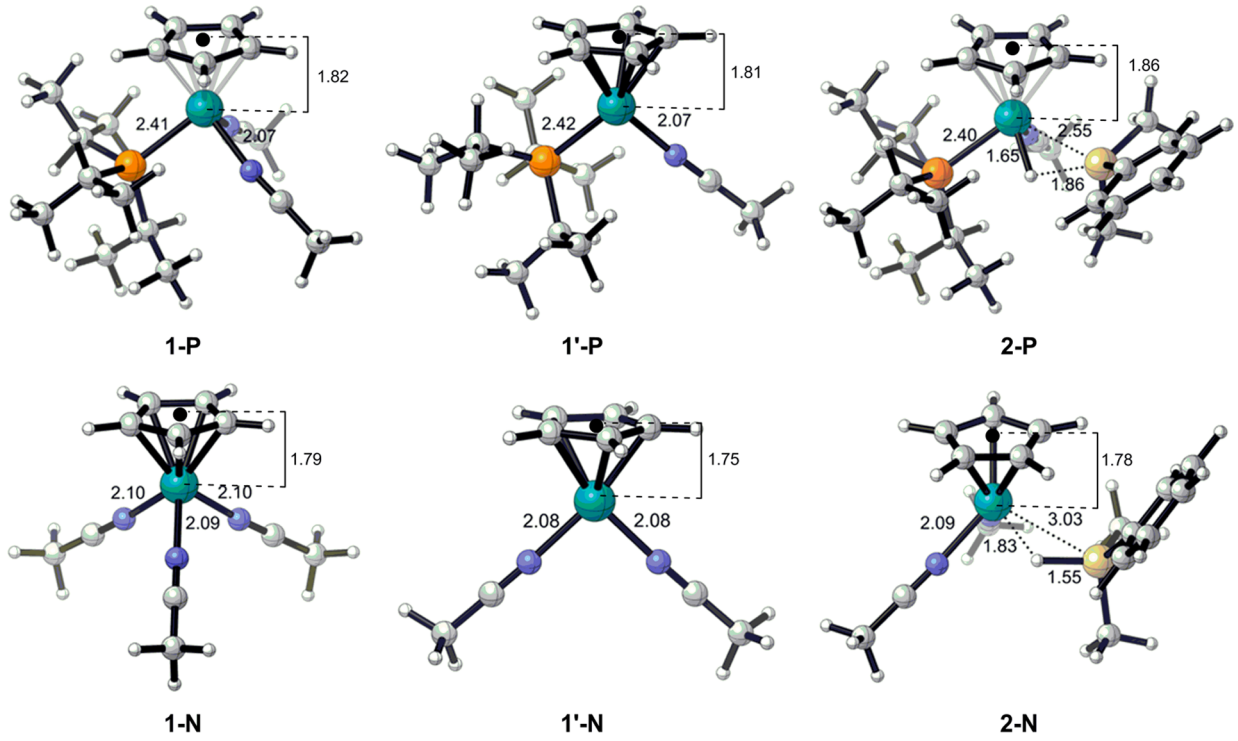

Figure 2. Structures of ruthenium complexes **1**, **1′**, and **2**.

reported that the catalyst **1-P**, an acetonitrile ligand of the Trost's catalyst **1-N** replaced by a phosphine ligand, also catalyzes the hydrosilylation of alkynes, giving the anti-Markovnikov product rather than the Markovnikov product (Scheme 2).[12]

Interestingly, catalyst **1-P** can also catalyze the hydrosilylations of acetone and acetonitrile,[12,13] but the hydrosilylations of acetone and nitriles catalyzed by **1-N** have not been reported (Scheme 2). The definitive mechanistic determinations of the process are relatively rare.[14,15] The alkyne hydrosilylation usually proceeds through the inner-sphere mechanism, in which the substrate coordinates to the metal center and is then attacked by the silyl group or hydride group on the metal center. An outer-sphere mechanism, S_N2-Si mechanism (substrate attacks the Si center), also occurs in some catalytic hydrosilylations. Whether the inner- or outer-sphere mechanism is plausible for hydrosilylation of other unsaturated compounds such as carbonyls and nitriles is still unclear (Scheme 3).

In view of extensive experimental developments and relatively rare theoretical studies, we undertook a systematic computational study to address the puzzling ligand effects on mechanisms of these hydrosilylation reactions.[16] We addressed the following four questions: (1) what are the operating mechanisms for alkyne substrates? (2) What is the origin of different selectivities observed for alkyne hydrosilylation by catalysts **1-P** and **1-N**? (3) What are the mechanisms of hydrosilylations of ketone and nitrile substrates? (4) Why is catalyst **1-P** active toward hydrosilylation of ketones and nitriles, while catalyst **1-N** is not?

■ COMPUTATIONAL METHODS

All the calculations were carried out with the Gaussian 09 package.[17] Geometry optimizations were performed with M06.[18,19] The Def2-TZVP basis set with the corresponding effective core potential[20] was used for Ru, and the 6-311G** basis set[21] was used for all other atoms. Frequency analysis was conducted at the same level of theory to verify the stationary points to be minima (zero imaginary frequency) or transition states (only one imaginary frequency) and to obtain zero-point energy (ZPE) and free energy corrections at 298.15 K. Single-point energies were calculated with the SMD[22] solvation model (solvent = chloroform or acetone). For the outer-sphere mechanism, due to the charge separation, the exact TS cannot be located in the gas phase, so full optimizations in acetone solvent at the same computational level were carried out to locate the TS. Intrinsic

dx.doi.org/10.1021/jo501730n | J. Org. Chem. 2014, 79, 8856−8864

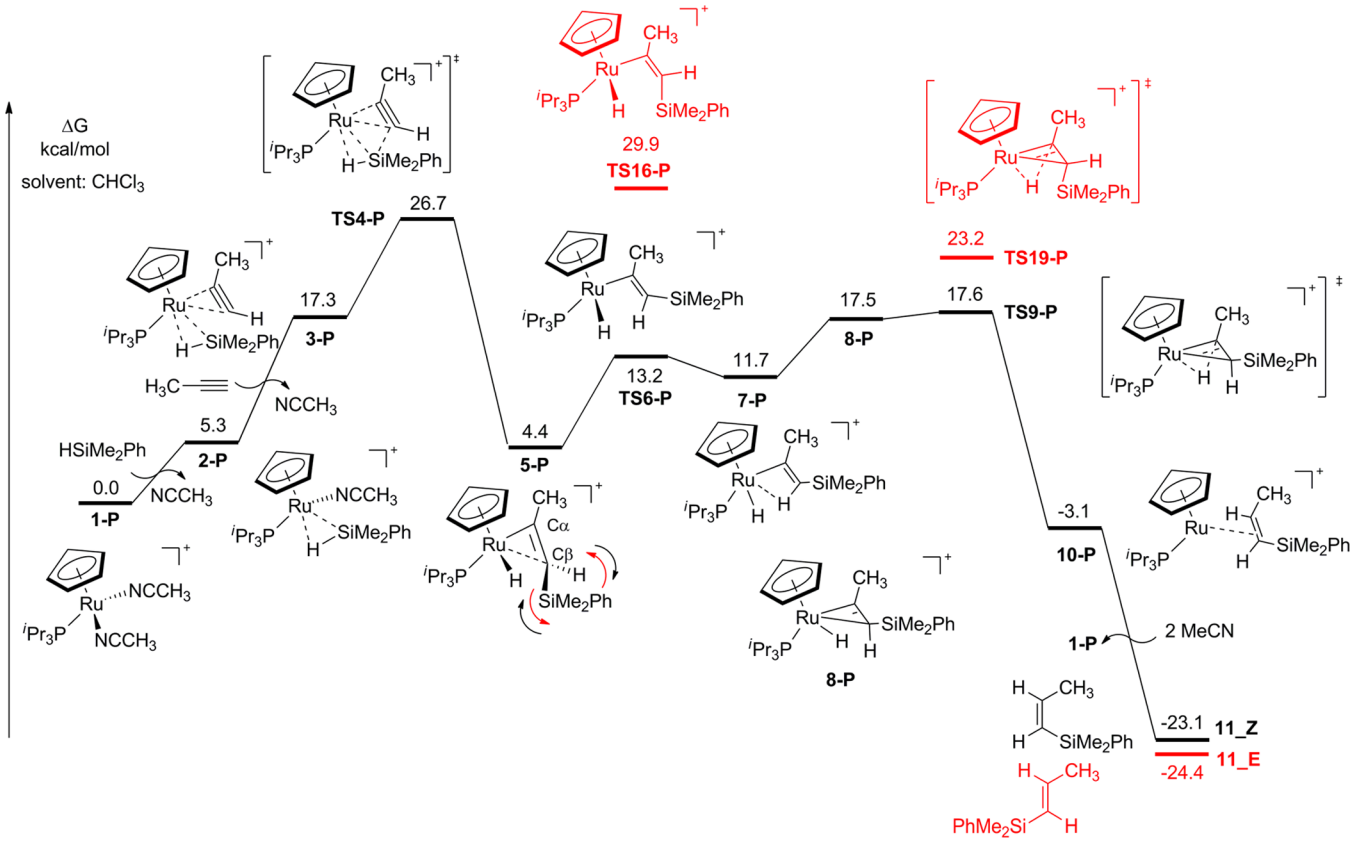

Figure 3. M06-computed free energy profile of propyne hydrosilylation with catalyst **1-P**. The relative free energies are given in kilocalories per mole. The black arrows in **5-P** represent the clockwise rotation of the C_α–C_β bond, whereas the red arrows represent the counterclockwise rotation of the C_α–C_β bond.

reaction coordinates (IRC) calculations[23] were performed to confirm that TS structures indeed connect two relevant minima. Computed structures are illustrated using CYLView.[24]

RESULTS AND DISCUSSION

Comparison of P^{i}Pr$_3$ and MeCN Ligands. The comparison of catalysts **1**, **1′**, and complex **2** provides deeper understanding of the effects of the phosphine and acetonitrile ligands. Dissociation of one acetonitrile ligand requires about 15.0 kcal/mol in the gas phase (7.0 kcal/mol in $CHCl_3$) for either catalyst **1-P** or **1-N**. This shows that the solvent can facilitate the dissociation of the acetonitrile ligand, as demonstrated by Houk and co-workers in a previous study.[25]

Figures 1 and 2 show the relative energies and the structures of catalysts, **1-P** and **1-N**, along with the results of dissociation of one acetonitrile to give **1′-P** and **1′-N** and the energies of these species with phenyldimethylsilane, **2-P** and **2-N**. Remarkably, a silane coordinates to **1′-P** and **1′-N** to form **2-P** and **2-N** in a η^2 or η^1 fashion, respectively. Compared to complex **2-N**, complex **2-P** displays a significantly longer H···Si distance (1.86 vs 1.55 Å) and shorter Ru···Si distance (2.55 vs 3.03 Å), indicating that the more basic P^{i}Pr$_3$ ligand facilitates the back-donation from the Ru center to the antibonding orbital of the Si–H bond,[2c,26−28] eventually breaking the Si–H bond. Acetonitrile is a more labile ligand to dissociate compared to that of the phosphine ligand. It can also be demonstrated by the preparation process that **1-P** can be easily obtained from a reaction of catalyst **1-N** with 1 equiv of phosphine ligand.[29] Therefore, the P^{i}Pr$_3$ ligand can facilitate formation of a η^2-silane complex by the mutual interactions of the ligand-to-metal σ bonding and back-donation from the metal, which are very important in activating the Si–H bond.[26] The bis-acetonitrile complex gives a less stable silane complex with weak coordination in solution.

Alkyne Hydrosilylation. Our previous theoretical studies on hydrosilylation of alkyne substrates with catalysts $[CpRu(MeCN)_3]^+$ (**1-N**) and $[Cp^*Ru(MeCN)_3]^+$ revealed a new pathway leading to the anti-addition and Markovnikov product.[10] Encouraged by this previous work, we computed the mechanism and selectivity of hydrosilylation of a propyne substrate with catalyst **1-P**, which is known to lead to the anti-Markovnikov product (Scheme 2).

Figure 3 gives the free energy profile for the most favorable reaction pathway. Catalyst **1-P** first undergoes ligand exchanges to form an intermediate **2-P** and then **3-P**, involving coordination of silane and propyne. The four possible transition states are shown in Figure 4 for silyl or hydride migration to either terminus of the propyne. **TS4-P**, in which the silyl group migrates to the β-carbon, is calculated to be the lowest-energy TS and also the rate-determining step, which controls the anti-Markovnikov regioselectivity. Analysis of these four TSs in Figure 4 reveals the origin of the regioselectivity. The NBO charge[28] (shown in Figure 4) on C_β is more negative than that on C_α due to the electron-donating effect of the methyl group of propyne. Therefore, the positively charged silyl group migration to C_β is more electronically favorable than migration to C_α. The two hydrogen migration TSs, **TS24-P** and **TS34-P**, are relatively unstable, also due to the steric clash between the bulky P^{i}Pr$_3$ and PhMe$_2$Si groups. In addition, the Si–H bond in **TS34-P** (2.08 Å) is shorter than that in **TS4-P** (2.54 Å). So,

dx.doi.org/10.1021/jo501730n | J. Org. Chem. 2014, 79, 8856−8864

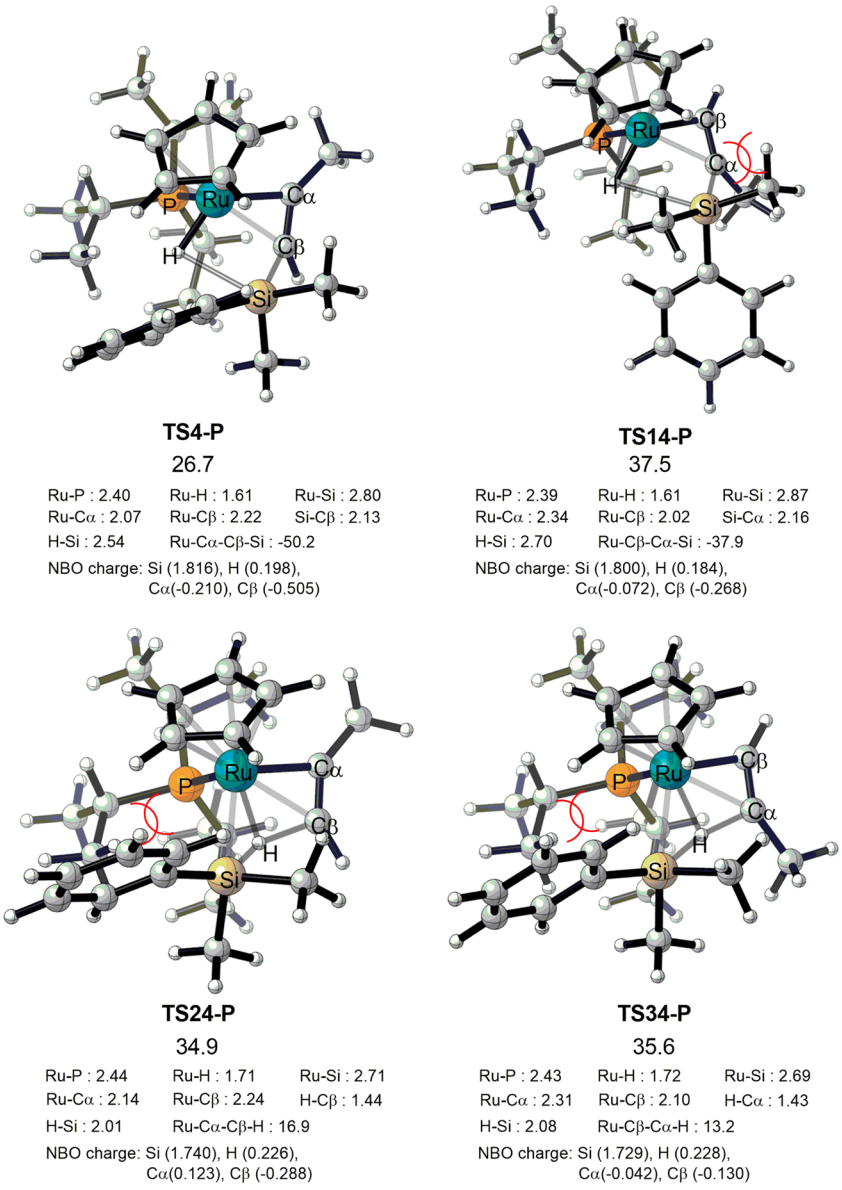

Figure 4. Four transition states of propyne hydrosilylation with catalyst **1-P**. The activation free energies are given in kilocalories per mole, and the bond lengths are shown in angstroms.

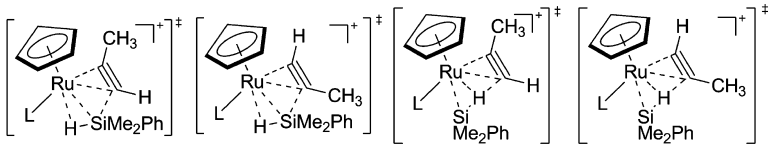

	TS4-L	TS14-L	TS24-L	TS34-L
L = P^iPr_3	**26.7**	37.5	34.9	35.6
L = MeCN	32.0	42.7	**22.1**	22.9
L = PMe_3	22.8	34.7	22.6	**21.5**

Figure 5. Transition states of propyne hydrosilylation catalyzed by the ruthenium catalysts $[Cp(L)Ru(MeCN)_2]^+$.

TS34-P is a much earlier transition state in which the Si−H bond is not better activated. Also, **TS14-P** is very unstable because of steric congestion between the silyl group and methyl group of propyne. The anti-Markovnikov and silyl migration pathway is the most energetically favorable one, since the steric hindrance among the bulky phosphine, silyl, and alkyl substituents on the alkyne is least severe.

We also located an 18-electron η^2-metallacyclopropene intermediate **5-P** derived from the silyl migration. The geometrical features of intermediate **5-P** suggest that the clockwise rotation of the $C_\alpha-C_\beta$ bond is more energetically favorable than the counterclockwise rotation; the clockwise rotation TS **TS6-P** is 16.7 kcal/mol lower than the counterclockwise rotation TS **TS16-P**. Finally, the α-H migration TS

dx.doi.org/10.1021/jo501730n | J. Org. Chem. 2014, 79, 8856−8864

TS9-P and a dissociation process lead to the anti-addition and anti-Markovnikov product.

We also investigated the outer-sphere mechanism for alkyne hydrosilylation. Calculations ruled out the alkyne attack on the silylium center, since it has a barrier of about 40 kcal/mol (see Supporting Information). Very recently, an alternative outer-sphere mechanism for the β-Z hydrosilylation of terminal alkynes with catalyst $[Ir(I)_2\{\kappa\text{-C,C,O,O-(bis-NHC)}\}]BF_4$ was reported.[30] The acetone solvent acts as a silane shuttle by transferring the silyl moiety from the silane to the alkyne. Migration of the silyl moiety to the acetone solvent is the first step of the alternative mechanism; this has a barrier of about 28.1 kcal with catalyst $[Cp(P^iPr_3)Ru(MeCN)_2]^+$. (See the following section for acetone hydrosilylation.) In addition, the solvent $CDCl_3$ was used in Nikonov's experiment. Therefore, only the inner-sphere mechanisms (hydrogen or silyl migration) operate for alkyne hydrosilylation in our case.

Effect of the Ligands. To further elucidate the role of the auxiliary ligand (L) on reactivity and selectivity, we studied the other two ligands, MeCN and PMe_3. The activation free energies are listed in Figure 5.

The less sterically demanding and basic ligand MeCN can accommodate the bulky adjacent silyl group. Also, a η^1-silane intermediate is formed, and the hydrogen migration TS **TS24-N** leading to the different (Markovnikov) product has the lowest barrier.[10] These calculation results are in agreement with the observed regioselectivity with this ligand. With the PMe_3 ligand, the hydrogen migration process is also favored. However, PMe_3 and MeCN prefer different regioselectivities for the hydrogen migration step: anti-Markovnikov for the PMe_3 ligand and Markovnikov for the MeCN ligand, respectively. The more basic PMe_3 ligand causes Ru to be more electron-rich and thus there is more back-donation to the H−Si bond. Consequently, the migrating hydrogen for the PMe_3 ligand should have more hydride character and prefer the α-position (anti-Markovnikov) than that of the MeCN ligand. These computational findings demonstrate that the ligand can play an important role in controlling the mechanism and regioselectivity through both electronic and steric factors (Scheme 4).

Acetone Hydrosilylation, Acetonitrile Hydrosilylation, and Ligand Effect. Both the inner- and outer-sphere pathways were studied to explore the possible mechanisms of hydrosilylation of acetonitrile and acetone. For the inner-sphere mechanisms, there are two possible pathways: initial hydrogen migration to the coordinated substrate via **TS64-L**[31] and **TS74-L** or initial silyl migration via **TS84-L** and **TS94-L**. Both of these pathways were found to have very high barriers of more than 30 kcal/mol. The outer-sphere mechanism can be regarded as a S_N2-Si mechanism, in which the substrate attacks the Si center followed by hydride migration to the silyl carbenium ion. This mechanism is similar to the recently reported ionic hydrosilylation pathway.[2d,32] A simple model for the hydrosilylation of acetone by $[CpRu(Me_3P)(MeCN)_2]^+$ was used and studied by DFT calculations by the Nikonov group.[13] Both studies support this S_N2-Si ionic mechanism as being the most favorable for hydrosilylation of acetones, although the computed barrier for our realistic ligand (**55-P**, 22.6 kcal/mol) is higher than the previously reported barrier (18.6 kcal/mol) for the simple model. These results are reasonable since the much more bulky P^iPr_3 ligand is used in our computational study.

The free energy profile of acetonitrile hydrosilylation catalyzed by **1-P** in acetone solvent is shown in Figure 6. The calculated results suggest that the S_N2-Si step is the rate-determining step and furnishes the neutral Ru-hydride intermediate and silylium ion (**45-P**). The second key step is hydride migration to the carbonium cation of the coordinated silylium ion through **TS47-P**, which gives intermediate **48-P**. Finally, the product dissociates from the metal center and regenerates the active catalyst. With regard to analogous ionic S_N2 reaction, the solvation effect is as important as steric effects.[33] As in the hydrosilylation of the nitrile, the acetone solvent was found to accelerate the reaction rate of hydrosilylation of acetonitrile.[13] It is challenging to locate the ionic S_N2 transition state, and we can locate this transition state only by geometry optimization in the solvent. On the basis of this result, we can estimate the free energy barrier of 27.6 kcal/mol for acetonitrile hydrosilylation in acetone solvent (shown in Figure 6), which is lower than that in chloroform solvent by 3.8 kcal/mol. Therefore, our studies are consistent with the experimental observation of an accelerating effect of acetone solvent.

We located the S_N2-Si transition states for catalyst **1-P** in acetone solvent with full optimization (Figure 7), but we could not locate transition states for the other catalysts such as **1-N**.[34] The S_N2-Si transition states, **TS44-P** for acetonitrile substrate and **TS54-P** for acetone substrate, have barriers of 27.6 and 28.1 kcal/mol, respectively. Our calculations underestimate the energy difference, since the hydrosilylation of nitriles can be done selectively in acetone as solvent.[12]

We also studied the ligand effects on the mechanisms of acetone hydrosilylation and acetonitrile hydrosilylation (Figure 8). The inner-sphere TS **TS64-L** cannot be located for the acetonitrile substrate, but **TS84-L** can be located. The bulky P^iPr_3 ligand is much more unfavorable than the PMe_3 ligand in the inner-sphere TSs **TS84-L** and **TS94-L**, due to the larger steric repulsion between the ligands and coordinated substrate. This can be demonstrated by the energy difference of their TSs **TS84-L** for acetonitrile substrate, 26.4 vs 30.4 kcal/mol for PMe_3 ligand vs P^iPr_3 ligand. The acetone substrate follows the same trend, 39.0 vs 46.8 kcal/mol for PMe_3 ligand vs P^iPr_3 ligand in **TS94-L**. In addition, as discussed in the Introduction, the P^iPr_3 ligand can strongly activate the Si−H bond and make the Si center easily attacked by the substrate in the outer-sphere mechanism. For the energetically favorable outer-sphere mechanism, the catalyst with the most bulky P^iPr_3 ligand has

Scheme 4. Propyne Hydrosilylation with Cationic Ruthenium Complexes $[CpRu(^iPr_3P)(MeCN)_2]^+$ (1-P) and $[CpRu(MeCN)_3]^+$ (1-N)

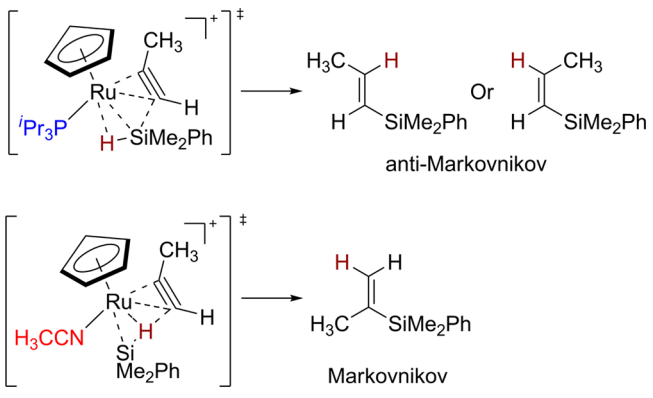

dx.doi.org/10.1021/jo501730n | J. Org. Chem. 2014, 79, 8856−8864

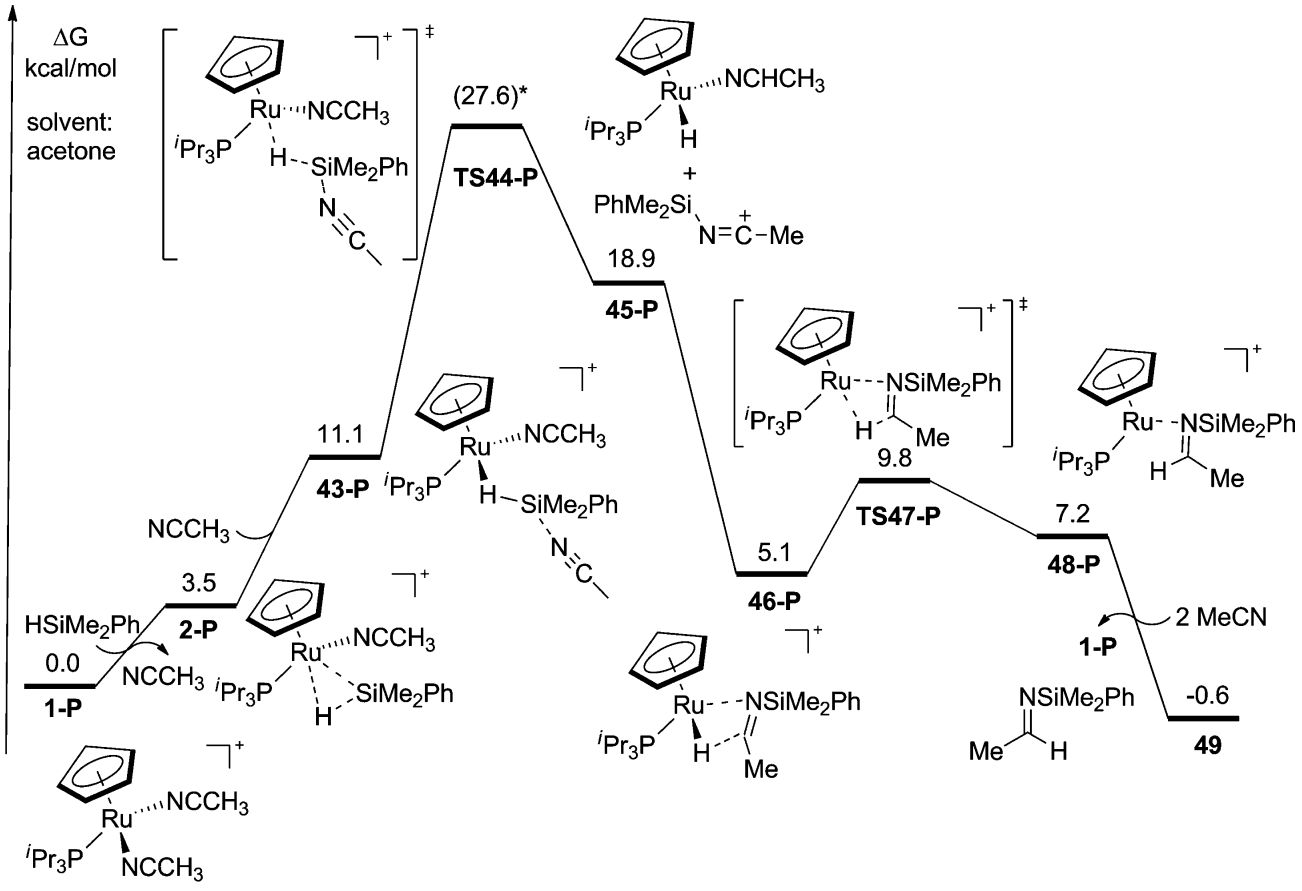

Figure 6. M06-computed free energy profile of acetonitrile hydrosilylation with catalyst **1-P**. The relative free energies are given in kilocalories per mole with single-point calculations in acetone solvent. *, see discussion of Figure 7.

TS44-P
27.6 kcal/mol

TS54-P
28.1 kcal/mol

Figure 7. Transition states of hydrosilylation of acetone and acetonitrile catalyzed by catalyst **1-P** obtained by full optimization in acetone solvent.

the lowest barrier compared to those with the MeCN and PMe_3 ligands, because it is beneficial from both its steric size and electronic effect. The inner-sphere mechanism is favorable for alkyne hydrosilylation, since alkyne is a good η-2 ligand, whereas acetonitrile and ketone substrates are better nucleophiles in the ionic mechanism than alkynes, but they are not a good η-2 ligand.

■ CONCLUSIONS

Our computations lead to the following conclusions about the ligand effects on the reactivity, selectivity, and mechanism of cationic ruthenium-catalyzed hydrosilylations of alkynes, ketones, and nitriles. First, in contrast to the η^1-silane intermediate formed by the silane addition to $[CpRu(MeCN)_3]^+$ (**1-N**), the catalyst $[Cp(^iPr_3P)Ru(MeCN)_2]^+$ (**1-P**) with a more basic P^iPr_3 ligand generates the η^2-silane intermediate and thus can facilitate Si−H bond activation to a greater extent. Second, for **1-P**-catalyzed alkyne hydrosilylation, it proceeds through the silyl migration first. Third, in contrast to the linear MeCN ligand, the larger P^iPr_3 ligand can push the large silyl group to migrate to C_β of propyne, resulting in the formation of anti-Markovnikov products. Fourth, for the case of hydrosilylation of ketone and nitrile catalyzed by **1-P**, the ionic S_N2-Si outer-sphere mechanism is the most favorable pathway.

dx.doi.org/10.1021/jo501730n | J. Org. Chem. 2014, 79, 8856−8864

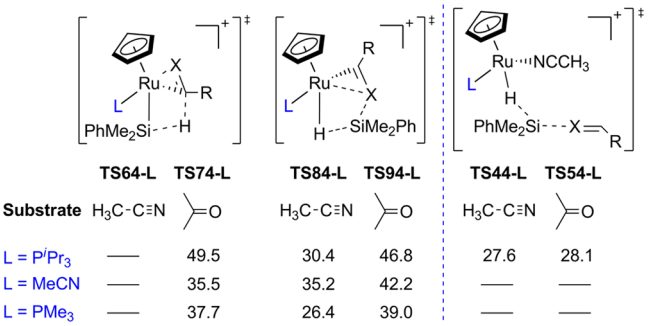

Figure 8. Transition states of hydrosilylation of acetone and acetonitrile catalyzed by ruthenium catalysts $[Cp(L)Ru(MeCN)_2]^+$ (L= P^iPr_3, MeCN, PMe_3) in acetone solvent. The inner-sphere TSs, **TS64-L**, **TS74-L**, **TS84-L**, and **TS94-L**, were obtained in gas optimization with single-point calculations in acetone solvent. The outer-sphere TSs, **TS44-L** and **TS54-L**, were obtained through full optimization in acetone solvent.

Although no definitive general conclusions apply to all of the systems and different catalysts/substrates may operate through different mechanisms, as shown in our studies, we believe that such a systematic study will provide insight into the development of catalytic hydrosilylation, an attractive strategy in organic synthesis.

■ ASSOCIATED CONTENT

Supporting Information

Cartesian coordinates and energies of all optimized structures. This material is available free of charge via the Internet at http://pubs.acs.org.

■ AUTHOR INFORMATION

Corresponding Authors

*(L.W.C.) E-mail: oscarchung@sustc.edu.cn.
*(K.N.H.) E-mail: houk@chem.ucla.edu.
*(Y.-D.W.) E-mail: wuyd@pkusz.edu.cn.

Notes

The authors declare no competing financial interest.

■ ACKNOWLEDGMENTS

We gratefully acknowledge financial support from the National Science Foundation of China (21133002, 21232001, 21302006), the MOST of China (2013CB911501), the Shenzhen Science and Technology Innovation Committee (KQTD201103, JCYJ20120614144601467), and the National Science Foundation of the United States (CHE-1059084).

■ REFERENCES

(1) (a) Ojima, I. In *The Chemistry of Organic Silicon Compounds*; Patai, S.; Rappoport, Z., Eds.; Wiley: New York, 1989; pp 1479−1526. (b) Ojima, I.; Li, Z.; Zhu, J. In *The Chemistry of Organic Silicon Compounds*; Rappoport, Z., Apeloig, Y., Eds.; Wiley: New York, 1998; Vol. 2, pp 1687−1792.

(2) (a) Miyashita, M.; Sasaki, M.; Hattori, I.; Sakai, M.; Tanino, K. *Science* **2004**, *305*, 495. (b) Corey, J. Y.; Braddock-Wilking, J. *Chem. Rev.* **1999**, *99*, 175. (c) Corey, J. Y. *Chem. Rev.* **2011**, *111*, 863. (d) Dioumaev, V. K.; Bullock, R. M. *Nature* **2000**, *424*, 530. (e) Yang, Y.-F.; Shi, T.; Zhang, X.-H.; Tang, Z.-X.; Wen, Z.-Y.; Quan, J.-M.; Wu, Y.-D. *Org. Biomol. Chem.* **2011**, *9*, 5845.

(3) (a) Corriu, R. J. P.; Moreau, J. J. E.; Pataud-Sat, M. *J. Organomet. Chem.* **1982**, *228*, 301. (b) Murai, T.; Sakane, T.; Kato, S. *J. Org. Chem.* **1990**, *55*, 449.

(4) (a) Hashimoto, H.; Watanabe, T.; Tobita, H. *J. Am. Chem. Soc.* **2006**, *128*, 2176. (b) Nikonov, G. I.; Peterson, E.; Khalimon, A. Y.; Sirnionescu, R.; Kuzmina, L. G.; Howard, J. A. K. *J. Am. Chem. Soc.* **2009**, *131*, 908. (c) Khalimon, A. Y.; Simionescu, R.; Kuzmina, L. G.; Howard, J. A. K.; Nikonov, G. I. *Angew. Chem., Int. Ed.* **2008**, *47*, 7701.

(5) (a) Gorin, D. J.; Sherry, B. D.; Toste, F. D. *Chem. Rev.* **2008**, *108*, 3351. (b) Hong, X.; Liang, Y.; Houk, K. N. *J. Am. Chem. Soc.* **2014**, *136*, 2017. (c) Zhou, J.-L.; Liang, Y.; Deng, C.; Zhou, H.; Wang, Z.; Sun, X.-L.; Zheng, J.-C.; Yu, Z.-X; Tang, Y. *Angew. Chem., Int. Ed.* **2011**, *50*, 7874.

(6) Ding, S.; Song, L.-J.; Chung, L. W.; Zhang, X.; Sun, J.; Wu, Y.-D. *J. Am. Chem. Soc.* **2013**, *135*, 13835.

(7) Hua, Y.; Nguyen, H. H.; Scaggs, W. R.; Jeon, J. *Org. Lett.* **2013**, *15*, 3412.

(8) Trost, B. M.; Ball, Z. T. *J. Am. Chem. Soc.* **2001**, *123*, 12726.

(9) (a) Chalk, A. J.; Harrod, J. F. *J. Am. Chem. Soc.* **1965**, *87*, 16. (b) Harrod, J. F.; Chalk, A. J. *J. Am. Chem. Soc.* **1965**, *87*, 1133.

(10) Chung, L. W.; Wu, Y. D.; Trost, B. M.; Ball, Z. T. *J. Am. Chem. Soc.* **2003**, *125*, 11578.

(11) (a) Rummelt, S. M.; Fürstner, A. *Angew. Chem., Int. Ed.* **2014**, *53*, 3626. (b) Sundararaju, B.; Fürstner, A. *Angew. Chem., Int. Ed.* **2013**, *52*, 14050. (c) Bernal, M. J.; Torres, O.; Martín, M.; Sola, E. *J. Am. Chem. Soc.* **2013**, *135*, 19008 and ref 6.

(12) Nikonov, G. I.; Gutsulyak, D. V. *Angew. Chem., Int. Ed.* **2010**, *49*, 7553.

(13) Gutsulyak, D. V.; Vyboishchikov, S. F.; Nikonov, G. I. *J. Am. Chem. Soc.* **2010**, *132*, 5950.

(14) Wu, Y.-D.; Wong, C.-L. *J. Org. Chem.* **1995**, *60*, 821.

(15) Miller, Z. D.; Li, W.; Belderrain, T. R.; Montgomery, J. *J. Am. Chem. Soc.* **2013**, *135*, 15282.

(16) (a) Zhang, X.-H.; Chung, L. W.; Lin, Z.; Wu, Y.-D. *J. Org. Chem.* **2008**, *73*, 820. (b) Chung, L. W.; Lee, H. G.; Lin, Z.; Wu, Y.-D. *J. Org. Chem.* **2006**, *71*, 6000. (c) Wu, Y.-D.; Chung, L. W.; Zhang, X.-H. In *Computational Modeling for Homogeneous and Enzymatic Catalysis*; Morokuma, K., Musaev, D. G., Eds.; Wiley-VCH: Weinheim, Germany, 2008; p 285.

(17) Frisch, M. J.; Trucks, G. W.; Schlegel, H. B.; Scuseria, G. E.; Robb, M. A.; Cheeseman, J. R.; Scalmani, G.; Barone, V.; Mennucci, B.; Petersson, G. A.; Nakatsuji, H.; Caricato, M.; Li, X.; Hratchian, H. P.; Izmaylov, A. F.; Bloino, J.; Zheng, G.; Sonnenberg, J. L.; Hada, M.; Ehara, M.; Toyota, K.; Fukuda, R.; Hasegawa, J.; Ishida, M.; Nakajima, T.; Honda, Y.; Kitao, O.; Nakai, H.; Vreven, T.; Montgomery, J. A., Jr.; Peralta, J. E.; Ogliaro, F.; Bearpark, M.; Heyd, J. J.; Brothers, E.; Kudin, K. N.; Staroverov, V. N.; Kobayashi, R.; Normand, J.; Raghavachari, K.; Rendell, A.; Burant, J. C.; Iyengar, S. S.; Tomasi, J.; Cossi, M.; Rega, N.; Millam, J. M.; Klene, M.; Knox, J. E.; Cross, J. B.; Bakken, V.; Adamo, C.; Jaramillo, J.; Gomperts, R.; Stratmann, R. E.; Yazyev, O.; Austin, A. J.; Cammi, R.; Pomelli, C.; Ochterski, J. W.; Martin, R. L.; Morokuma, K.; Zakrzewski, V. G.; Voth, G. A.; Salvador, P.; Dannenberg, J. J.; Dapprich, S.; Daniels, A. D.; Farkas, O.; Foresman, J. B.; Ortiz, J. V.; Cioslowski, J.; Fox, D. J. *Gaussian 09*, revision A.02; Gaussian, Inc.: Wallingford, CT, 2009.

(18) Zhao, Y.; Truhlar, D. G. *Theor. Chem. Acc.* **2008**, *120*, 215.

(19) M06 was found to perform well in describing binding behavior, which is important for the metal−ligand interaction. For benchmark examples, see (a) Ahlquist, M. S. G.; Norrby, P.-O. *Angew. Chem., Int. Ed.* **2011**, *50*, 11794. (b) Chen, P.; Dougan, B. A.; Zhang, X.; Wu, Y.-D.; Xue, Z.-L. *Polyhedron* **2013**, *58*, 30.

(20) (a) Andrae, D.; Häußermann, U.; Dolg, M.; Stoll, H.; Preuß, H. *Theor. Chim. Acta.* **1990**, *77*, 123. (b) Weigend, F.; Ahlrichs, R. *Phys. Chem. Chem. Phys.* **2005**, *7*, 3297.

(21) Krishnan, R.; Binkley, J. S.; Seeger, R.; Pople, J. A. *J. Chem. Phys.* **1980**, *72*, 650.

(22) Marenich, A. V.; Cramer, C. J.; Truhlar, D. G. *J. Phys. Chem. B* **2009**, *113*, 6378.

(23) (a) Fukui, K. *Acc. Chem. Res.* **1981**, *14*, 363. (b) Fukui, K. *J. Phys. Chem.* **1970**, *74*, 4161.

(24) Legault, C. Y. *CYLView*, 1.0b; Université de Sherbrooke: Sherbrooke, Quebec, Canada, 2009; http://www.cylview.org.

(25) Hong, X.; Trost, B. M.; Houk, K. N. *J. Am. Chem. Soc.* **2013**, *135*, 6588.
(26) (a) Lin, Z. *Chem. Soc. Rev.* **2002**, *31*, 239. (b) Nikonov, G. I. *Adv. Organomet. Chem.* **2005**, *53*, 217. (c) Sakaki, S.; Takayama, T.; Sumimoto, M.; Sugimoto, M. *J. Am. Chem. Soc.* **2004**, *126*, 3332.
(27) The Wiberg bond index (WBI) suggests that the smaller bond order of Si−H in **2-P** compared to that in **2-N** (0.259 vs 0.579) also indicates a weaker Si−H bond and a larger extent of activation of Si−H in **2-P**. The WBI of Ru−Si (0.393 vs 0.148) again demonstrates that **2-P** is a η^2-silane complex and **2-N** is a η^1-silane complex. For natural bond orbital (NBO) analysis, see ref 28.
(28) (a) Reed, A. E.; Weinstock, R. B.; Weinhold, F. *J. Chem. Phys.* **1985**, *83*, 735. (b) Reed, A. E.; Curtiss, L. A.; Weinhold, F. *Chem. Rev.* **1988**, *88*, 899.
(29) (a) Osipov, A. L.; Gutsulyak, D. V.; Kuzmina, L. G.; Howard, J. A. K.; Lemenovskii, D. A.; Süss-Fink, G.; Nikonov, G. I. *J. Organomet. Chem.* **2007**, *692*, 5081. (b) Trost, B. M.; Frederiksen, M. U.; Rudd, M. T. *Angew. Chem., Int. Ed.* **2005**, *44*, 6630. (c) Kündig, E. P.; Monnier, F. R. *Adv. Synth. Catal.* **2004**, *346*, 901.
(30) Iglesias, M.; Sanz Miguel, P. J.; Polo, V.; Fernández-Alvarez, F. J.; Pérez-Torrente, J. J.; Oro, L. A. *Chem.—Eur. J.* **2013**, *19*, 17559.
(31) Unfortunately, the hydrogen migration TS **TS64-L** cannot be located when using catalyst **1-N**.
(32) (a) Gu, P.; Wang, W.; Wang, Y.; Wei, H. *Organometallics* **2013**, *32*, 47. (b) Yang, J.; White, P. S.; Brookhart, M. *J. Am. Chem. Soc.* **2008**, *130*, 17509. (c) Du, G.; Fanwick, P. E.; Abu-Omar, M. M. *J. Am. Chem. Soc.* **2007**, *129*, 5180.
(33) Chen, X.; Regan, C. K.; Craig, S. L.; Krenske, E. H.; Houk, K. N.; Jorgensen, W. L.; Brauman, J. I. *J. Am. Chem. Soc.* **2009**, *131*, 16162.
(34) Despite taking either the H−Si or Si−X bond distance as the reaction coordinate, the gas-phase energy profiles went uphill without a barrier (see Supporting Information), which is similar to the recent computational study of rhenium(V)-oxo complex-catalyzed carbonyl hydrosilylation reported by Wei and co-workers (ref 32a).